Angle-dependent oscillations in valence-band photoemission intensity of C_{60}

2007 J. Phys.: Condens. Matter 19 026202

(http://iopscience.iop.org/0953-8984/19/2/026202)

INSTITUTE OF PHYSICS PUBLISHING JOURNAL OF PHYSICS: CONDENSED MATTER

J. Phys.: Condens. Matter **19** (2007) 026202 (8pp) doi:10.1088/0953-8984/19/2/026202

Angle-dependent oscillations in valence-band photoemission intensity of C_{60}

S He[1], M Arita[1], H Namatame[1], M Taniguchi[1,2], H-N Li[3] and H-Y Li[3]

[1] Hiroshima Synchrotron Radiation Center, Hiroshima University, Higashi-Hiroshima, Hiroshima 739-8526, Japan
[2] Graduate School of Science, Hiroshima University, Higashi-Hiroshima 739-8526, Japan
[3] Department of Physics, Zhejiang University, Hangzhou 310027, People's Republic of China

E-mail: shephy@hiroshima-u.ac.jp (Shaolong He)

Received 31 August 2006, in final form 24 November 2006
Published 15 December 2006
Online at stacks.iop.org/JPhysCM/19/026202

Abstract

High-resolution angle-resolved photoelectron spectroscopy (ARPES) has been performed to investigate valence-band photoemission in C_{60} single crystals, which were cleaved in ultra-high-vacuum systems. The results present angle-dependent modulations in intensities of valence-band photoemission of the C_{60} single crystal. The observed intensity modulations are caused by polarization influence and photoelectron diffraction (PED) effects, of which the latter is also responsible for the similar oscillations produced by varying incident photon energies. The calculated results indicate that only photoelectrons scattered by the top hemisphere of C_{60} molecules dominate the angle-dependent interference modulations.

1. Introduction

The fullerenes, in particular C_{60} [1], are a very interesting class of materials with many unexpected characters and behaviours. For example, the valence-band photoemission spectra of C_{60} thin films have exhibited interesting oscillations in intensities when the incident photon energies varied [2]. It was suggested by Benning *et al* [2] that the well defined intensity oscillations of the highest- and next-highest-occupied-molecular-orbital- (HOMO- and NHOMO-) derived bands of the C_{60} solid are due to transitions to final states that retain distinct molecular character and symmetry. Following this observation, similar oscillations have been also found in photoemission spectroscopy (PES) measurements of gas phase C_{60} [3], high fullerenes C_{86} [4], heterofullerenes $C_{59}N$ [5], and a C_{60} monolayer on an Ag single crystal [6]. Very recently, Becker *et al* [7] performed detailed experiments with smaller steps and higher photon energies to study the oscillating behaviours in C_{60}. In a previous work [8], we have also measured the intensity modulations of the lowest-unoccupied-molecular-orbital- (LUMO-) derived band in rare-earth-doped fullerene films.

Theoretically, the first successful model concerning this unique phenomenon was proposed by Xu *et al* from the three-step model of photoemission theory [9]. They had calculated the photoionization matrix element of the C_{60} molecule using the spherical wavefunctions of initial and final states, and hence predicted the correct photon energies, where the minimum of photoionization cross section occurred. The more detailed and quantitative calculated result was reported by Hasegawa *et al* [10]. By taking account of the scattering effects of the photoelectron waves emanating from the 60 carbon atoms, they found the numerical calculated results in good agreement with the measured spectrum lines. Their calculations revealed that, due to the spherical structure of the C_{60} molecule as well as its large radius, the photoelectron diffraction (PED) effects in C_{60} molecules dominated the intensity oscillations.

The well defined oscillations in the HOMO (NHOMO) of C_{60} still deserve to be investigated in detail. In a C_{60} molecule, the electron cloud of the π-derived HOMO and NHOMO is delocalized over a volume of well defined spherical shell. The frequencies of the oscillations are related to the geometric properties of the C_{60} molecule's π electron cloud, such as thickness and diameter [11]. This provides us with an opportunity to extract this information from the measured photoionization cross section oscillations, hence have a better understanding of the C_{60} electronic structures [7]. Meanwhile, the reason for the exact opposite phase in oscillations of HOMO and NHOMO, as the main feature of the phenomenon, is still elusive. Benning *et al* suggested that the opposite phase modulations in intensity of HOMO and NHOMO, which are odd (*ungerade*) and even (*gerade*) in symmetry respectively, can be explained by initial- and final-state symmetry and parity selection rules [2]. However, a calculation using a molecular orbital with alternating symmetries and free-electron-like final states failed to describe the observed oscillations even qualitatively [12].

Regarding the PED effects, intensity oscillations can be achieved by varying the incident photon energies (and thereby the kinetic energies of the emitting photoelectrons) while leaving the detection geometry constant. This is the case described above. An alternative mode is to fix the incident photon energy (hence fix final state kinetic energy). The interference of photoelectrons is then measured by changing the azimuth and/or polar detection angle of photoelectrons. Indeed, the angle- and polarization-dependent photoelectron spectra of C_{60} polycrystalline films have been recently reported by Schiessling *et al* [13]. The intensity of HOMO- and NHOMO-derived bands showed variation with both the changes of emission and polarization angle. They found that the variations in photoionization cross section of the C_{60} solid can be described by an asymmetry parameter of free molecules. Their observations demonstrate the validity of applying the calculated results on free molecules to experimental results on C_{60} solids. However, they did not take into account the PED effects, which definitely exist in photoemissions of C_{60} and have dominated the observed photon-energy-dependent oscillations in intensity. In order to clarify the influence of PED effects on the angular distribution (AD) of C_{60} solids, we should take the AD measurements not only in a much smaller angle step but also with different incident photon energies.

In this paper, we present the measured results of angle-dependent photoelectron intensities of the C_{60} valence band. The polarization influence and the so-called hemisphere structure factor of C_{60} molecules have been calculated. The results provide us with a qualitative explanation of the experimental observations. In the meantime, we carried out high-resolution ARPES of a C_{60} single crystal at room temperature and below 260 K, where the orientation order–disorder transition occurs [14]. The ARPES results of simple cubic (sc) ordered phase below 260 K remain the same as that of the face-centred cubic (fcc) phase. There is no observable band dispersion either in the HOMO- or NHOMO-derived band of the C_{60} single crystal even at a low temperature.

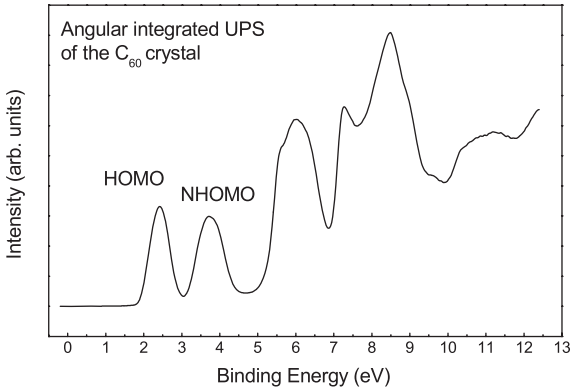

Figure 1. Angular integrated UPS of the C_{60} single crystal at 23 eV photon energy.

2. Experiment

The C_{60} single crystals were prepared by the gas phase method [15]. One of the free (111) surfaces with size of $\backsim 4 \times 5$ mm^2 was cemented to the sample holder with silver glue, while the other parallel (111) surface cemented with a post was used to cleave in vacuum. To avoid charging effects, the sample was fully covered by conductive glue. ARPES measurements were performed after the single crystal was cleaved in vacuum with a base pressure better than 9×10^{-11} Torr at undulator beamline BL9A of the storage ring at the Hiroshima Synchrotron Radiation Center (HSRC). An off-plane Eagle monochromator with a 1200 lines mm^{-1} spherical grating and the SES2002 analyser were used to collect the ARPES spectra. The angular parameters were kept at the incidence of photons $\alpha = 50°$ and the take-off angle of photoelectrons varied from $-15°$ to $15°$ with respect to the surface normal. The overall energy and angle resolution in the experiment are about 10 meV and 0.3°, respectively. Binding energy was defined with respect to E_F, which was determined from the spectra of the Au film. The cleaved surface proved to be (111) and the edge to be (110) after the experiment.

3. Results and discussion

3.1. ARPES measurements of C_{60} single crystals

The angular integrated ultraviolet photoemission spectrum (UPS) of the C_{60} single crystal obtained at room temperature is shown in figure 1, in which incident photon energy $\hbar\omega$ is 23 eV. The positions and shapes of the HOMO and NHOMO in figure 1 are very similar to the earlier data taken from polycrystalline films [16], which indicates that the charging effects of the C_{60} crystal at room temperature can be neglected. The valence-band features of the C_{60} solid retain distinct molecular orbital character when compared with the gas phase photoemission data [3]. In figure 1, the relative intensity of NHOMO and HOMO valence band, which have fivefold and ninefold degeneracy respectively, does not reflect their occupied electron number ratio (5/9), but its dependence on the detection angle of photoelectrons according to the following discussion.

We carried out high-resolution ARPES on the cleaved (111) surface of the C_{60} single crystal in detail by varying the sample temperature and incident photon energies. The experimental data from both the normal and off-normal emissions were mainly collected approximately along the high-symmetry direction. The ARPES spectra in figure 2, which

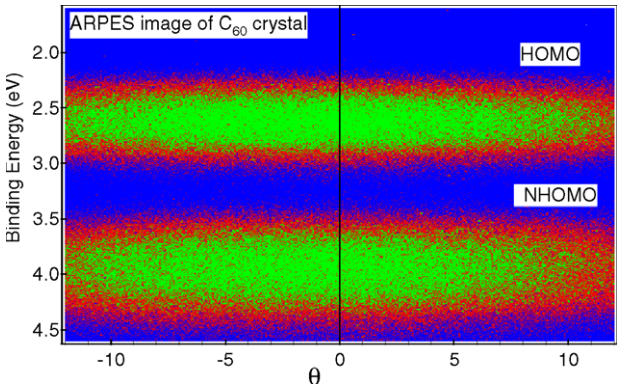

Figure 2. ARPES image of the C_{60} crystal taken at 23 eV photon energy. Polar detection angles ϑ (degrees) are measured from the surface normal.

(This figure is in colour only in the electronic version)

were obtained at room temperature with photon energy $\hbar\omega = 23$ eV, indicate that the energy dispersions of the C_{60} crystal photoemission features are very small, which confirms the results reported by Wu *et al* [12]. In spite of the high-resolution (both in energies and $k_{\|}$) photoemission spectroscopy employed in the experiments, we failed to exhibit any resolved structure in the HOMO and NHOMO valence bands, even at a low temperature. Unlike the well resolved band dispersion in the LUMO-derived band of metal-doped C_{60} [17, 18], dispersion in the HOMO and NHOMO of the C_{60} solid, which was predicted by band calculations [19], remains uncertain. These results indicate clearly that neither the orientational disorder nor the $k_{\|}$ resolution could be the reason for hindering the observations of dispersions [12, 20]. The lack of band dispersions both in our measurements and the work of Wu *et al* also indicates that the electronic structures of well defined C_{60} single crystals are somewhat different from crystalline film samples, since the latter show a dispersion of the order of 400 meV in the HOMO-derived band [21, 22]. The resolution of degree of band dispersions in undoped solid C_{60} is very important and thus calls for further ARPES measurements with single crystals and theoretical consideration for its clarification. The band width (FWHM) of the HOMO-derived band determined by angle-integrated and angle-resolved photoemission at room temperature yields nearly the same value, about 0.48 ± 0.01 eV, which is close to the results of thin films [23] and those of the LDA calculations [19, 24, 25], but much smaller than the ARPES results on single crystals [26].

While the observed photoemission line shapes show small changes over a wide range of crystal momentum ($k_{\|}$), intensities of valence band spectra of C_{60} exhibit unusual oscillations. Figure 3 depicts the relative photoelectron intensity of the NHOMO valence band, determined by spectrum lines normalized to the area of the HOMO (the method of extracting relative intensity was described in detail in an earlier work [8]), as a function of the polar detection angle with respect to the surface normal. Since the energy dispersions in the valence band are very small, such intensity variations are not genuinely related to the properties of solid C_{60}. As a result of the molecular nature of C_{60} solid, polarization effects strongly influenced the main trend of intensity variation presented in figure 3 [13]. Also, this is responsible for the AD asymmetry with respect to the surface normal [13]. However, light polarization influence could not explain all the features of intensity modulations depicted in figure 3 by itself, since it generally tends to produce gradual intensity variation with emission angle, rather than the well

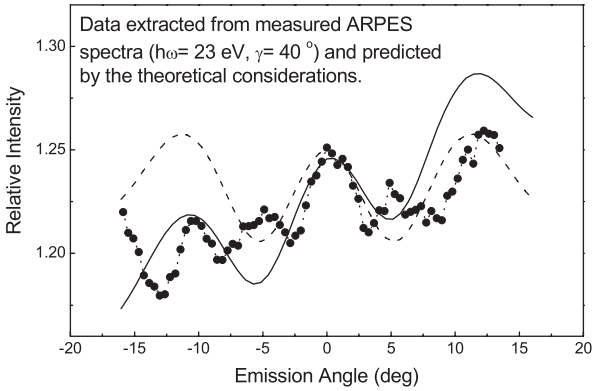

Figure 3. Photoemission intensity modulations of the NHOMO-derived band of the C_{60} single crystal as a function of emission angle ϑ measured from the surface normal. γ denotes the angle between the polarization vector and surface normal. The solid circles represent the relative intensities of the NHOMO level extracted from the ARPES spectra, which were normalized to the area of the HOMO level. The dotted line between solid circles is to guide the eyes. The calculated results by the hemisphere approximation following the polarization influence are respectively plotted in dashed and solid curves.

defined oscillations in figure 3 [22]. The angle-dependent oscillations shown in figure 3 are thought to have originated from the PED effects within a C_{60} molecule, which could explain the similar valence-band intensity modulations of C_{60} produced by varying incident photon energies [10]. The PED effects can be treated only in one C_{60} molecule for the following reasons. First, since the diameter of the C_{60} molecule is larger than the photoelectron's inelastic mean-free path (IMFP) with a photon energy range of 10–100 eV, UPS can only detect the top layer of the C_{60} sample [27–29]. Second, both experimental [2, 3] and calculated results [9–11] reveal that only the intramolecular scattering is significant. Indeed, the emitting photoelectron waves, which are elastically scattered by other C_{60} molecules, are attenuated by both the r^{-2} law and inelastic scattering and thus can be safely neglected. Below we will demonstrate why the measured results in figure 3 could be well interpreted in terms of PED effects as well as polarization influence.

3.2. Comparison between calculated and experimental results

First we consider the PED effects. The photoelectrons emitting from a C_{60} molecule are scattered by the 60 carbon atoms and produce interference due to the phase difference of each wave. In photoemission spectroscopy, the analyser is sufficiently far from the sample as compared with the wavelength of photoelectrons, and the structure factor $S(k_f)$ is given by [14]

$$S(k_f) = \sum_j f_j \exp(-i\vec{k}_f \cdot \vec{r}_j), \tag{1}$$

where f_j and $\vec{r}_j$ are the atomic form factor and position of the jth atom related to the molecular centre. The supposed plane wavevector $\vec{k}_f$ of emitting photoelectrons is related to the photoelectron kinetic energy E_k and the centrifugal potential U_0 by $k_f = \sqrt{2m_e(E_k - U_0)}/\hbar$. Due to the random orientational rotating of C_{60} molecules at room temperature, we assume that the 60 carbon atoms of C_{60} form the surface of a sphere of radius R ($\approx$3.54 Å) on which they spread smoothly over the sphere. In addition we have a cloud of the 240 valence electrons

(each carbon atom supplies four) in a hollow sphere centred around the cage of the carbon ions and the thickness of the electron cloud Δ is close to the length of C–C covalent bond. The emitting photoelectrons are thus scattered by the electron cloud formed by both the charges of the carbon ion cores and their valence electrons. Therefore, the structure factor of the C_{60} molecule becomes

$$S(k_f) \propto f_e \int_0^{2\pi} d\varphi \int_0^{\pi} d\theta \sin\theta \exp(-i\vec{k}_f \cdot \vec{r}), \tag{2}$$

in which f_e is the scattering radius of an electron and $r = R + \Delta$.

However, the angle-dependent oscillations cannot be expected from equation (2) due to the spherical symmetry of C_{60} molecules. In order to explain the experimental data depicted in figure 3, we suppose that only photoelectron waves scattered by the top hemisphere of a C_{60} molecule are significant in photoelectron interference. Hence, one gets the structure factor of the hemispherical C_{60} molecule

$$S(k_f) \propto f_e \int_0^{2\pi} d\varphi \int_0^{\frac{\pi}{2}} d\theta \sin\theta \exp(-ik_f r(\cos\varphi \sin\theta \sin\vartheta + \cos\theta \cos\vartheta)), \tag{3}$$

where ϑ is the polar detection angle with respect to the surface normal. By selecting a proper value of Δ and the potential U_0, the angle-dependent modulations could be explained qualitatively by this simple model. In figure 3, the numerical calculated results are plotted against ϑ, where Δ is set to be 0.96 Å and $U_0 = 58.7$ eV.[4] Rough as this approximation appears to be, it can still predict the main period of the angle-dependent oscillations presented in figure 3. Deviations of the calculated result from the experimental data at $\vartheta = \pm 5^\circ$ might be due to two aspects of the above approximations, which attempt to make the calculations feasible in this work. First, we assumed that the 60 carbon atoms are distributed homogeneously on the C_{60} sphere. In fact, the atomic density distribution on the molecular sphere is nonuniform [30]. Second, we supposed that the density of valent electrons is uniform over the C_{60} molecule. This may also wash out some fine structures in the calculated results presented in figure 3. In order to make the calculations more accurate, we have to use the electronic density distribution determined by their wavefunctions instead of a uniform valence electron cloud.

One of the main features of the experimental data (solid circle) in figure 3 is that the intensities are not symmetric with respect to the surface normal. However, the above calculation result is obviously symmetric (dashed line). In order to explain this, we include the influence of polarization on AD mentioned above. If the polarization of incident synchrotron radiation light is considered, the photoionization cross section can be approximated by [31, 32]

$$\frac{d\sigma(k_f)}{d\Omega} = \frac{\sigma}{4\pi}[1 + \beta P_2(\cos\phi)]|S(k_f)|^2, \tag{4}$$

where σ is the total cross section for ionization of an electron, and ϕ the angle between the direction of polarization and the direction of the outgoing photoelectrons' momentum. P_2 represents the Legendre polynomial of second order and β denotes the energy-dependent asymmetry parameter of the molecular orbital (MO). $S(k_f)$ has been determined by equation (3). Thus equation (4) defines the AD of photoelectrons relative to the direction of polarization of the incident light. For a photon energy of 23 eV, the value of asymmetry parameter for the NHOMO of the C_{60} molecule is determined to be $\beta \approx 0.1$ from the calculated results of Decleva *et al* [33]. Because of the good agreement between their calculated results

[4] This value of U_0 in C_{60} molecules is much larger than the inner potential of C_{60} solids, which is estimated to be within 20 eV. However it is still smaller than the value of 78 eV in [9] used to fit the experimental data. The centrifugal potential changes rapidly inside the hollow molecule and its value only reflects the potential within the shell (its thickness = Δ). The physical interpretation of U_0, should not be overemphasized.

and experimental data, we adopt this value in our calculation. Meanwhile, in our ARPES measurements, the light polarization angle is about 40° with respect to the surface normal and ϕ in equation (4) is therefore determined by $\phi = 40 - \vartheta$ (ϑ is defined in equation (3)). The later calculated result depicted in figure 3 (solid curve) can well explain the asymmetry of the experimental data with surface normal and is in better agreement with the experimental data than the dotted curve.

Considering the hemisphere model's simple approximation made here, its ability to predict the main features of experimental data is quite impressive. We shall give brief remarks on its physical foundation. In C_{60} solids, the photoelectrons' IMFP, which was determined to be about 4 or 5 Å with kinetic energies ranging from 20 to 50 eV in C_{60} solids [23, 29], is close to the molecular radius (∼3.54 Å). Therefore, photoelectrons scattered by the bottom hemisphere of the C_{60} molecule are significantly attenuated and their contribution to the photoemission spectra can be neglected. In this sense, the hemisphere approximation seems to be, in principle, reasonable.

4. Conclusion

High-resolution ARPES spectra of the C_{60} single crystal's valence band show little energy dispersion in HOMO- and NHOMO-derived bands even at a low temperature. Our results indicate that the lack of dispersion in these bands might reflect the exact nature of the electronic structures of C_{60} single crystals (at least of their surface layers).

In addition, ARPES spectra of the valence band exhibit angle-dependent oscillations in valence emission intensities. The observed intensity modulations are due to PED effects and polarization influence during the photoemission process. We suppose that the emitting photoelectrons scattered by the top hemisphere of C_{60} molecules contribute significantly to the interference oscillations. A simple calculation based on this approximation and polarization influence can explain the main features of the observed oscillations very well. It is believed that the oscillations contain detailed information on geometric structures of the C_{60} molecule such as the MO's asymmetry parameter, molecular size and even the exact thickness of the valence electron cloud. More detailed and quantitative calculations and experimental measurements are desired to completely understand the intensity oscillations of the C_{60} valence band caused either by varying the incident photon energies or detection polar angles.

Acknowledgments

This work has been supported by the National Natural Science Foundation of China under contract Nos 10074053 and 10374080. One of the authors (S He) would like to thank Professor Y B Xu and S Qiao for their stimulating discussion.

References

[1] Kroto H W, Heath J R, O'Brien S C, Curl R F and Smally R E 1985 *Nature* **318** 162
[2] Benning P J, Poirier D M, Troullier N, Martins J L, Weaver J H, Haufler R E, Chibante L P F and Smalley R E 1991 *Phys. Rev.* B **44** R1962
[3] Liebsch T, Plotzke O, Heiser F, Hergenhahn U, Hemmers O, Wehlitz R, Viefhaus J, Langer B, Whitfield S B and Becker U 1995 *Phys. Rev.* A **52** 457
[4] Hino S, Umishita K, Iwasaki K, Miyazaki T, Kikuchi K and Achiba Y 1996 *Phys. Rev.* B **53** 7496
[5] Jones F H, Butcher M J, Cotier B N, Moriarty P, Beton P H, Dhanak V R, Prassides K, Kordatos K, Tagmatarchis N and Wudl F 1997 *Phys. Rev.* B **59** 9834
[6] Ton-That C, Shard A G, Egger S, Dhanak V R and Welland M E 2003 *Phys. Rev.* B **67** 155415

[7] Rüdel A, Hentges R, Becker U, Chakraborty H S, Madjet M E and Rost J M 2002 *Phys. Rev. Lett.* **89** 125503
[8] He S L, Li H N, Wang X X, Li H Y, Xu Y B, Bao S N, Ibrahim K, Qian H J, Su R, Zhong J, Hong C H and Abbas M I 2005 *Phys. Rev.* B **71** 085404
[9] Xu Y B, Tan M Q and Becker U 1996 *Phys. Rev. Lett.* **76** 3538
[10] Hasegawa S, Miyamae T, Yakushi K, Inokuchi H, Seki K and Ueno N 1998 *Phys. Rev.* B **58** 4927
[11] Frank O and Rost J M 1997 *Chem. Phys. Lett.* **271** 367
[12] Wu J, Shen Z X, Dessau D S, Cao R, Marshall D S, Pianetta P, Lindau I, Yang X, Terry J, King D M, Wells B O, Elloway D, Wendt H R, Brown C A, Hunziker H and de Vries M S 1992 *Physica* C **197** 251
[13] Schiessling J, Kjeldgaard L, Balasubramanian T, Nordgren J and Brühwiler P A 2003 *Phys. Rev.* B **68** 205405
[14] Heiney P A 1992 *J. Phys. Chem. Solids* **53** 1333
[15] Tan M, Xu B, Li H, Qi Z and Xu Y 1997 *J. Cryst. Growth* **182** 375
[16] Li H, He S, Zhang H, Lu B, Bao S, Li H, He P and Xu Y 2003 *Phys. Rev.* B **68** 165417
[17] Yang W L, Brouet V, Zhou X J, Choi H J, Louie S G, Cohen M L, Kellar S A, Bogdanov P V, Lanzara A, Goldoni A, Parmigiani F, Hussain Z and Shen Z X 2003 *Science* **300** 303
[18] Brouet V, Yang W L, Zhou X J, Choi H J, Louie S G, Cohen M L, Goldoni A, Parmigiani F, Hussain Z and Shen Z X 2004 *Phys. Rev. Lett.* **93** 197601
[19] Saito S and Oshiyama A 1991 *Phys. Rev. Lett.* **66** 2637
[20] Antropov V P, Gunnarsson O and Liechtenstein A I 1993 *Phys. Rev.* B **48** 7651
[21] Gensterblum G, Pireaux J J, Thiry P A, Caudano R, Buslaps T, Johnson R L, Le Lay G, Aristov Günther R, Taleb-Ibrahimi A, Indlekofer G and Petroff Y 1993 *Phys. Rev.* B **48** R14756
[22] Benning P J, Olson C G, Lynch D W and Weaver J H 1994 *Phys. Rev.* B **50** R11239
[23] Wertheim G K 1995 *Phys. Rev.* B **51** R10248
[24] Ching W Y, Huang M Z, Xu Y N, Harter W G and Chan F T 1991 *Phys. Rev. Lett.* **67** 2045
[25] Shirley E L and Louie S G 1993 *Phys. Rev. Lett.* **71** 133
[26] He P, Bao S, Yu C and Xu Y B 1995 *Surf. Sci.* **328** 287
[27] Tjeng L H, Hesper R, Heessels A C L, Heeres A, Jonkman H T and Sawataky G A 1997 *Solid State Commun.* **103** 31
[28] Wertheim G K, Buchanan D N E, Chaban E E and Rowe J E 1992 *Solid State Commun.* **83** 785
[29] Goldoni A, Sangaletti L, Parmigiani F, Comelli G and Paolucci G 2001 *Phys. Rev. Lett.* **87** 076401
[30] Chow P C, Jiang X, Reiter G, Wochner P, Moss S C, Axe J D, Hanson J C, McMullan R K, Meng R L and Chu C W 1992 *Phys. Rev. Lett.* **69** 2943
[31] Cooper J W and Manson S T 1969 *Phys. Rev.* **177** 157
[32] Fano U and Cooper J W 1968 *Rev. Mod. Phys.* **40** 441
[33] Venuti M, Stener M, De Alti G and Decleva P 1999 *J. Chem. Phys.* **111** 4589